JOURNAL OF MATERIALS SCIENCE 31 (1996) 2501–2514

Review
Solders in electronics

W. J. PLUMBRIDGE

Materials Discipline, The Open University, Walton Hall, Milton Keynes, MK7 6AA, UK

The metallurgy and mechanical behaviour of the principal solder types based on lead–tin alloys are reviewed. Particular emphasis is placed upon their performance under simulated service conditions, fatigue, creep and ageing, and life prediction. Requirements for improved and more environmentally compatible solders are explored.

1. Introduction

Soldering may be defined as "a process by which metals may be joined via a molten metallic adhesive (the solder) which on solidification forms strong bonds (usually intermetallic compounds) with the adherents". It is generally regarded as being restricted to alloys with a liquidus temperature below 400 °C.

Although the technique has been used since Roman times, it is only in the last few decades that the performance of soldered joints in electrical and electronic devices has received detailed attention. Now, with electronics shortly to become the largest industrial sector and an estimated output of some 10^{13} joints per annum [1], solders and soldered joints are regarded as pivotal to future developments in electronics. It is not simply their ubiquity that produces this greater interest. As a consequence of continuing miniaturization and ever-increasing performance demands, their reliability is becoming more severely tested in service. While, hitherto, it was sufficient to prescribe solders on the basis of their processability (flow, wetting, chemical characteristics) the structural integrity of the joint, and hence the mechanical behaviour of solders, has become of equal importance. In addition, from the environmental perspective, there are twin pressures to eliminate lead from solders and atmospheric pollutants from the cleaning and fluxing processes. It is therefore not surprising that there has been an explosion in research interest on this general topic in recent years.

After a brief outline of the service situation, the article will examine the metallurgical, mechanical and structural aspects of solder joints. Emphasis will be placed on: (1) the two most common generic solder types, eutectic lead-tin and "high" lead lead-tin alloys and (ii) joints produced in surface mount technology (SMT) which have a definite structural role and which are predicted to constitute 80% of all components by 2000 AD [2].

With respect to life prediction and reliability in service, the extent to which existing methodologies currently used for high temperature structural alloys (e.g. low alloy steels for steam power plant, nickel-base alloys for gas turbines) may be applied to solder joints, will be explored.

2. Joints and solders

Soldering is the preferred method for attaching components to printed circuit boards (PCBs) or chips to substrates. On traditional boards the integrated circuit is packaged in a dual-in-line package and solder attached into the holes in the board. A surface mount assembly is a composite structure of the printed circuit board, the solder joint and the surface mount component. Unlike traditional through-hole technology, SMT has smaller components which are soldered directly to the pad surface of the PCB. The solder joint is the sole mechanical means of attaching the component to the PCB, in addition to acting as the electrical connection and often, the means of heat dissipation. SMT allows components to be mounted on both sides of the board. Schematic examples of typical joint configurations are shown in Fig. 1. The solder bump is commonly used to connect a silicon chip to an alumina substrate and is employed in benign environments. Die or substrate geometries may incorporate several layers to accommodate thermal strain, especially with the increasing trend for greater interfacial areas. Leadless (i.e. without leads *not* lead, Pb) chip carriers are most vulnerable to thermal strains because of their structural rigidity whereas this problem is reduced by the incorporation of compliant leads in leaded chip carriers. In practice, selection of connection types or combinations is determined by manufacturing, electronic and service considerations.

Apart from low liquidus temperatures, alloys for solders to be used in an electronic assembly require a narrow melting range (preferably less than 10 °C). Common binary systems include tin–lead, tin–silver, tin–antimony, tin–indium, tin–bismuth and lead–indium alloys. Ternary alloys include tin–lead with silver, gold, bismuth, indium or antimony additions. A selection of compositions and properties is

0022–2461

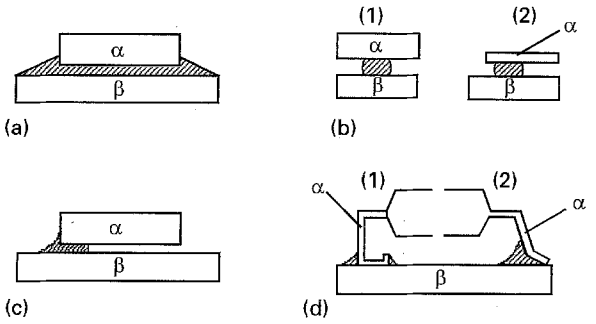

Figure 1 Some common solder joint configurations [2]. Shaded area is solder and α, β are different materials.

presented in Table I. In practice, the variety of solders is enormous but, in terms of usage and our knowledge and understanding of their behaviour, two groups are relevant: (i) tin–lead alloys at, or near, the eutectic composition (37 wt % lead) and (ii) lead rich, tin–lead alloys with compositions around 5 wt % tin.

3. Service conditions

The principal influences encountered by joints in service are thermal fluctuations and, to a much lesser extent, mechanical vibrations. Two sources arise for the former: heat generated within the devices themselves, which is a growing problem as the push towards further miniaturization continues, and temperature changes which stem from the external operating environment. According to the application these variations may be quite substantial (Table II). The values cited here exclude the contribution from heat dissipation from the device, and the fluctuation in temperature, ΔT, is smaller than the difference between maximum and minimum temperature values due to seasonal or geographic variations. As a consequence of these conditions and the marked differences in the coefficients of thermal expansion of the materials used for the component, substrate and solder (Table III), thermal strains are developed in the joint which are cyclic in nature. Frequency is governed by the frequency of switching of the device and the interval between environmental changes. The process is shown schematically in Fig. 2. Solders are usually much softer than the other joint components and the majority of the strain generated is concentrated within the thin layer of solder adhesive. For many joint types, especially the leadless variety, the service conditions may best be approximated to strain controlled fatigue in shear. It is also salient that the levels of strains

TABLE I Compositions and properties of solders

Alloy composition (wt %)	Liquidus (°C)	Solidus (°C)	Tensile strength (MPa)	0.2% Proof strength (MPa)	Uniform elongation (%)
63Sn–37Pb	183	183	35.4	16.1	1.4
60Sn–40Pb	190	183	28.0	14.2	5.3
25Sn–75Pb	266	183	23.1	14.2	8.4
10Sn–90Pb	302	268	24.3	13.9	18.3
5Sn–95Pb	312	308	23.2	13.3	26.0
80Sn–20Pb	199	183	43.2	29.6	0.8
42Sn–58Bi	138	138	66.9	41.6	1.3
70Sn–30In	175	117	32.2	17.5	2.6
95Sn–5Ag	240	221	55.8	40.4	0.84
40Sn–60In	122	113	7.6	4.6	5.5
95Sn–5Sb	240	235	56.2	38.1	0.85
95Pb–5In	314	292	25.2	13.9	33.0
70Pb–30In	253	240	33.3	24.7	15.1
95Pb–5Sb	295	252	25.6	16.9	13.7
85Pb–10Sb–5Sn	255	245	38.4	25.3	3.5
88Pb–10Sn–2Ag	290	268	27.2	15.5	15.9
97.5Pb–1Sn–1.5Ag	309	309	38.5	29.9	1.15
85Sn–10Pb–5Sb	230	188	44.5	25.0	1.40

TABLE II Temperature limits and performance requirements for electronic assemblies

Application	T_{min} (°C)	T_{max} (°C)	ΔT (°C)	Dwell (h)	Cycles (per year)	Lifetime (years)
Consumer	0	60	35	12	365	1–3
Computers	15	60	20	2	1460	≃ 5
Telecommunications	−40	85	35	12	365	7–20
Commercial Aircraft	−55	95	20	2	3000	≃ 10
Motor Vehicle (Passenger Compartment)	−55	65	40	12	100	≃ 10
Motor Vehicle (Engine Compartment)	−55	125	100	1	300	≃ 5
Space (low earth orbit)	−40	85	35	1	8760	5–20
Military Avionics	−55	95	60	2	500	≃ 5

TABLE III Coefficients of thermal expansion for materials used in electronic assemblies

Material	Expansion coefficeint ($\times 10^{-6}\,K^{-1}$)
Solder(63Sn–37Pb)	22
Solder (95Pb–5Sn)	28.7
Solder (96.5Sn–3.5Ag)	22
Alumina	6.5
Aluminium nitride	2.7
Copper	16.7
Silicon	2.5
Epoxy resin	26

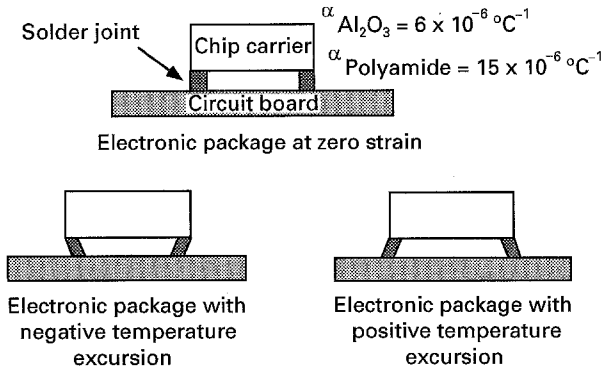

Figure 2 Development of strains in an electronic device (after Morris *et al.* [4]).

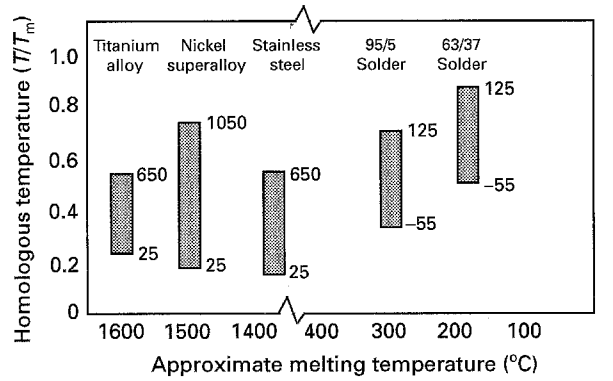

Figure 3 Comparison of homologous temperatures for engineering alloys in typical service conditions.

developed often exceed 10% and, as such, are an order of magnitude greater than those commonly encountered in most other structural alloys employed, for example, in power generation.

However, this is only part of the story. The inherent low melting point of solders, necessary for economy and to avoid damage to other joint elements, has a disadvantage in that room temperature represents a high homologous temperature. (The homologous temperature T_h of a material is the ratio of a current temperature, say, in operation, to the melting point–both temperatures being expressed in degrees Kelvin). Fig. 3 indicates the severity of typical service conditions for solders (T_h up to 0.9 T_m) as compared with other "high" temperature structural alloys. The consequence of solders experiencing more arduous conditions near room temperature than say a nickel-

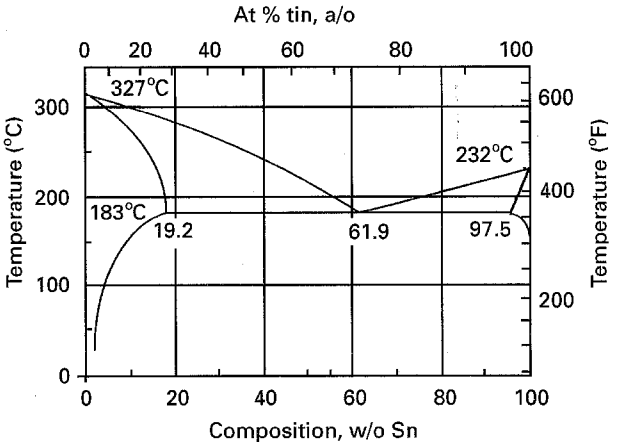

Figure 4 The lead–tin phase diagram.

base superalloy at above 1000 °C is somewhat difficult to appreciate. It does, however, mean that *time dependent* effects such as creep, stress relaxation, surface and microstructural changes, in addition to purely cyclic phenomena, must be taken into account in both testing and life prediction. Power on/power off, or environmental change cycles, are typically of the order of several hours or a few days, and it is the form of the mechanical hysteresis loop developed by these cycles that determines endurance in 80% of joint failures in service [3].

4. Metallurgy and microstructure of lead–tin solder alloys

With information regarding other solder alloy systems being fragmentary and dispersed, it is appropriate to focus upon the lead–tin system. Here, two quite metallurgically different groups of alloys are of interest. Of paramount importance is the eutectic (37 wt % lead) or near-eutectic group and, for higher melting point applications, lead-rich (between 90 and 97.5% lead) alloys. In the following paragraphs attention will be concentrated on those factors governing performance rather than a comprehensive exposition of the physical metallurgy involved or detailed descriptions of ternary and higher alloys.

The lead–tin phase diagram is shown in Fig. 4. Slow cooling of eutectic alloys from the liquid produces a lamellar microstructure of alternate layers of lead-rich and tin-rich phases (Fig. 5(a)). Areas of lamellae of similar orientation are known as colonies. In general, the colony size and interlamellar spacing decrease with increasing cooling rate and eventually a spheroidal structure replaces the lamellar arrangement (Fig. 5(b)). Proeutectic dendrites of either lead-rich or tin-rich phases exist in off-eutectic alloys. Joints in electronic connections are essentially castings produced under poorly controlled and variable conditions, and may contain a range of microstrutures. Lead-rich solders exist as a single phase solid solution at temperatures in excess of about 100 °C and attain an equilibrium two-phase structure at room temperature after a period of several days [4]. It is significant that the solvus temperature falls into the service band which may result in dissolution–reprecipitation reactions

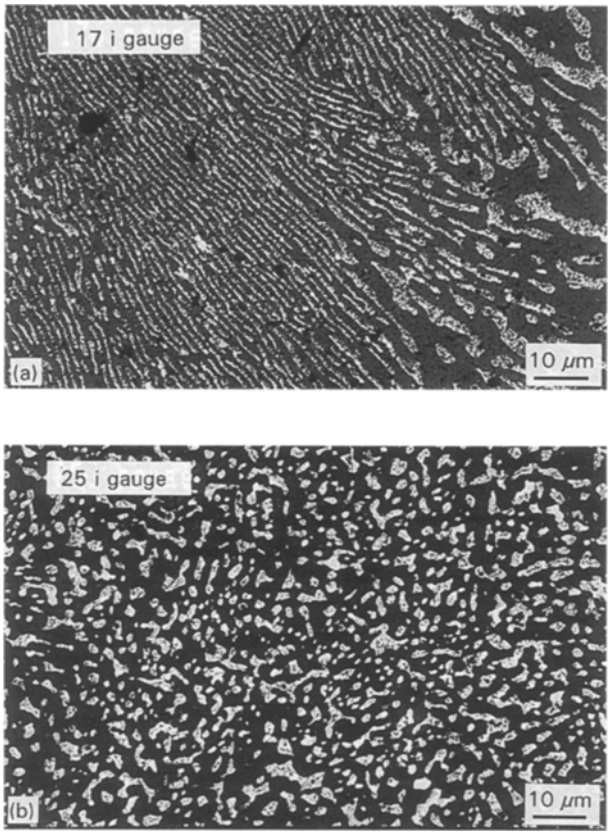

Figure 5 (a) Microstructure of a eutectic lead–tin alloy after slow cooling. (b) Microstructure of a eutectic lead–tin alloy after rapid cooling.

during alternate heating and cooling. While some workers suggest that the microstructural instability is sufficient for the effects of prior history to be readily eliminated [5, 6], others contend that such evidence persists for many years in service [7].

Due to the high homologous temperature both alloy types are unstable even after slow cooling. In eutectic alloys the eutectic grains, and any tin-rich precipitates within the lead-rich matrix, coarsen significantly and this is associated with a fall in shear strength [8]. In the lead-rich category, discontinuous cellular precipitation or homogeneous precipitation of tin-rich β phase occurs according to the cooling rate [9]. An approximate doubling of strength may be developed between zero and total transformation [4] but this is likely to be accompanied by an equivalent fall in ductility. Under the action of stress microstructural instability is enhanced. Recrystallization and the formation of equiaxed lead-rich and tin-rich phases occur (Fig. 6).

Damage resulting from cyclic stresses or strains is usually concentrated into recrystallized and coarsened bands in eutectic alloys when the original colony structure is destroyed and replaced by equiaxed α and β phase particles (Fig. 7). As with precipitate strengthened aluminium alloys this coarse, soft, band further localizes deformation until a crack is formed which ultimately leads to fracture. At low strain ranges ($\Delta\varepsilon_t < 0.3\%$) this banding is absent and fatigue failure arises due to the development and growth of intergranular cracks [10]. In contrast, cyclic failure

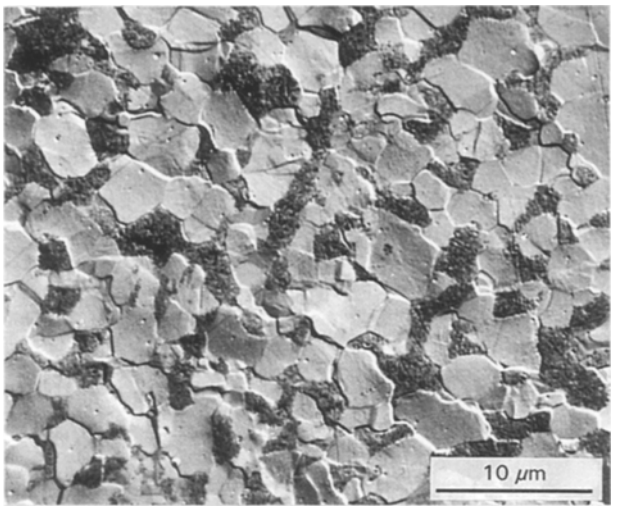

Figure 6 Worked and annealed 60Sn–40Pb alloy producing equiaxed lead-rich and tin-rich grains.

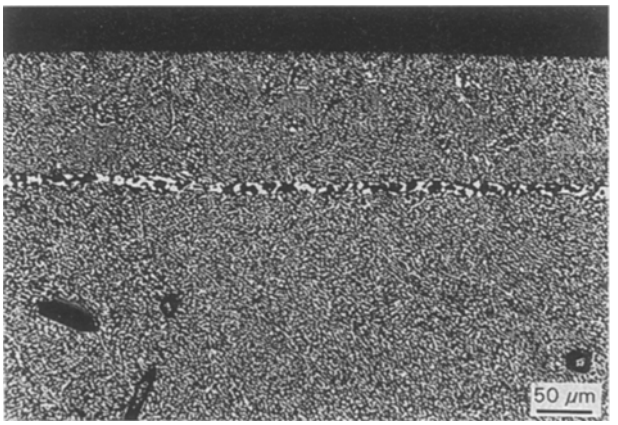

Figure 7 Microstructural coarsening in a 60Sn–40Pb alloy resulting from isothermal fatigue [69]. (Courtesy D. Tribula).

mechanisms in lead-rich solders involve intergranular fracture arising from grain boundary sliding or intersecting slip bands, or crack initiation at inclusions [11]. Broadly similar failure mechanisms to the above operate in each solder group during thermal and thermomechanical fatigue [12]. Continuous cycling is rarely experienced in service. The operating pattern contains dwells during which opportunities for time-dependent damage processes, such as creep cavitation, are enhanced.

Consideration of the metallurgy of the joint, as opposed to the solder alone, reveals a further important microstructural feature. Interaction between the solder and the base metal during soldering produces "intermetallics" which constitute the bond. The initial thickness of the intermetallic layer is dependent upon the production route for each joint type. These brittle materials may extend into the solder either by needle-like growth or by detached fragments from the main body of the intermetallic. Further growth may occur during service and result in enbrittlement of the joint. Since soldered joints are essentially thin layers of solder strained in shear, the arrangement and size of the intermetallics may have a profound effect on overall joint behaviour. Cracking often occurs along, or within, the intermetallic layer. Common examples of

TABLE IV Values of Young's modulus for solders

Alloy	Modulus (GPa)	Reference
60Sn–40Pb	38.6 ± 4	79
	16	80
	15	81
	30	82
	35	83
63Sn–37Pb	32	60
	30–34	84
	5.7	85
	20.5	86
95Pb–5Sn	26	60
96.5Sn–3.5Ag	24	60

intermetallics include Cu_3Sn and Cu_6Sn_5 for eutectic solders on a copper substrate, Cu_3Sn for high-lead solders on copper and Au–Sn and Au–Sn_2 for eutectic alloys on a gold substrate [13].

5. Mechanical behaviour of solders

The following paragraphs briefly review the mechanical behaviour of solders. Emphasis is placed upon those factors which are most influential in determining the service performance of soldered joints.

Because room temperature represents a high homologous temperature, lead–tin solders are soft and extremely deformable under ambient conditions. Under the action of a single monotonic stress they can exhibit elastic, anelastic and viscoplastic behaviour. True elasticity is often difficult to isolate and this has produced a wide variation in reported values for Young's modulus (Table IV). Quite substantial variations in modulus as a function of strain rate have been reported [4] (Fig. 8) although it is difficult to reconcile these from the phenomenological standpoint. However, since deviations from true elastic behaviour occur at strains below 0.05%, it is understandable why such findings have been made. High strain rates and low stress levels are required to minimize time dependent effects. An empirical expression for the temperature variation of Young's modulus for eutectic solders is [14]

$$E = -0.088(T\,^{\circ}\mathrm{C}) + 32\ \mathrm{GPa}$$

Reliable values of modulus are essential for stress analysis purposes, but in the case of soft solders, the dilemma exists whether to use an absolute value or an effective value which accommodates the prevailing strain rate. The overall stress–strain response is also sensitive to strain rate with substantial increases in strength and ductility resulting from higher strain rate testing [16] (Fig. 9). Tensile strength, σ, has been related to strain rate, $\dot{\varepsilon}$, via a power function relationship

$$\sigma = A\dot{\varepsilon}^{1/N}$$

where A and N are constants. In keeping with the greater potential for time dependent effects, differences in strain rate become more influential with increasing temperature [16]. Superplasticity develops with the

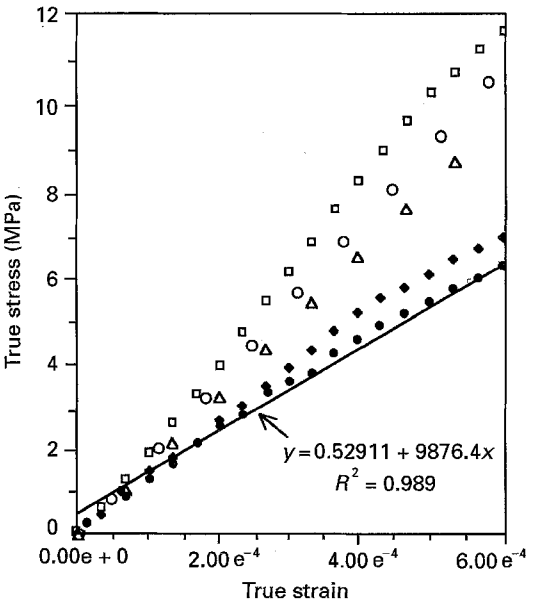

Figure 8 Effect of strain rate on initial deformation of a near-eutectic solder alloy. (amended from [14]). Strain rates ● 0.00017, ♦ 0.00017, □ 0.017, ○ 0.017, △ 0.017.

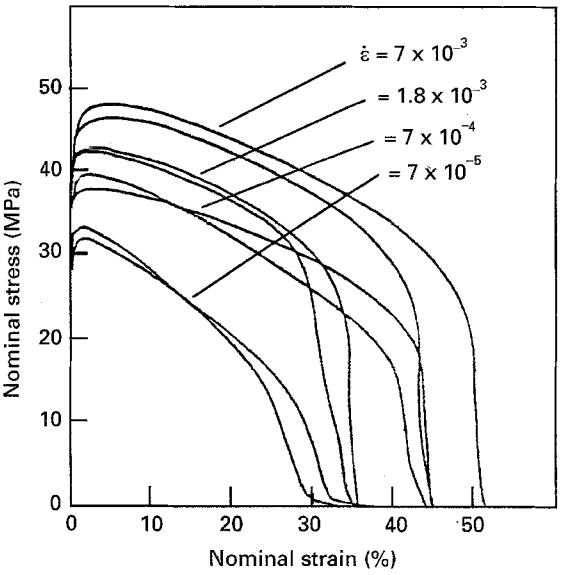

Figure 9 Influence of strain rate on overall stress–strain response of a eutectic alloy at room temperature [16].

appropriate combination of grain size, temperature and strain rate.

Much of the mechanical property data produced on solders involves reference to the speed of crosshead displacement of the test machine. The results produced are thus *configuration-specific* (i.e. dependent upon both the stiffness of the machine and the dimensions of the specimen). Even assuming a perfectly rigid loading frame, the actual strain rates experienced by the specimen when controlled by crosshead displacement are inversely proportional to the gauge length. Comparison of data from different sources is difficult and, further, it is important to note that it is the *material-specific* strain rate sensitivity which is required in constitutive equations for use in stress analysis.

The shear strength of rapidly cooled eutectic alloys has been shown to be some 20% greater than after

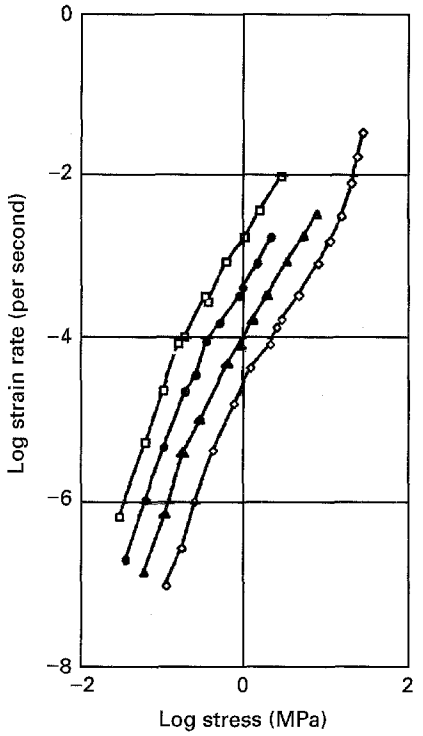

Figure 10 Creep strain rate versus stress relationship for a eutectic solder. □ 149 °C; ●119 °C; ▲ 88 °C; ◇ 63 °C. $g = 5.8$ μm. (After F. A. Mohamed and T. G. Langdon, *Phil. Mag.* **32** (1975) 697).

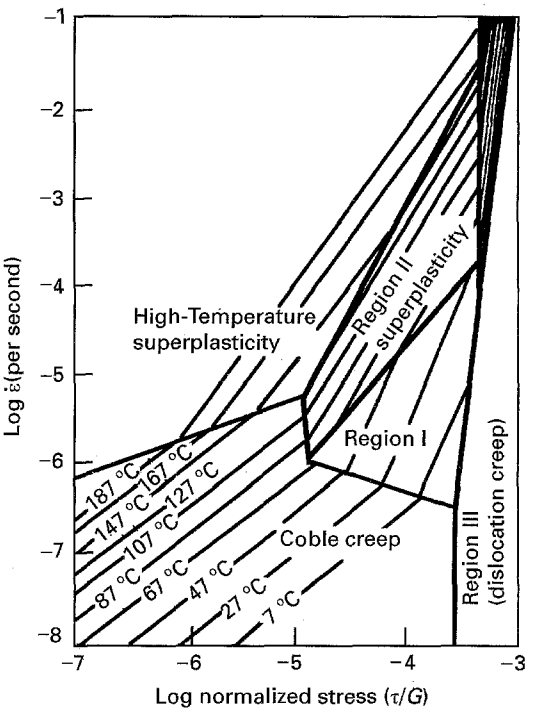

Figure 11 Deformation mechanism map for a eutectic solder [19]. $g = 5.5$ μm.

slow cooling. However, room temperature ageing for 30 days was sufficient to eliminate this difference [5] as the microstructures merged.

5.1. Creep

The presence of hold periods in the service cycle provides opportunities for creep (under stress controlled conditions) or stress relaxation (when strain limits are fixed) to occur. Considering that for the eutectic solder, room temperature represents a homologous temperature of 0.65, and operation at 140 °C is equivalent to a T_h of 0.90, it is understandable why time-dependent mechanical processes are so important. While a considerable amount of data is available describing creep in eutectic solder alloys [17] much of it relates to high steady-state strain rates ($> 10^{-4}\ s^{-1}$) which are rarely encountered in service. Over a range of strain rates between 10^{-7} and $10^{-2}\ s^{-1}$ the relationship between applied stress and steady state (or minimum) creep rate on a log–log basis is generally described as sigmoidal (Fig. 10) and results from three interacting mechanisms. As with all creep data from different sources, considerable scatter arises due to differences in processing, microstructure, impurity levels and testing procedures. For example, deformation rates under the same stress may change by up to threefold following prior strain or microstructural alteration [18]. A deformation mechanism map for a eutectic alloy with a grain size of 5.5 μm is shown in Fig. 11 [19]. In Region 1, the low stress regime, the stress exponent is about 3, while in the superplastic region (Region 2) it falls to between 1.6 and 2.4. Under high stresses (Region 3) the stress exponent has been found to vary between 3 and 16. Deformation in Regions 1 and 2 exhibits an inverse grain size dependence whereas this microstructural feature has little influence on deformation in Region 3 [17]. Preliminary findings regarding the influence of microstructure, produced under different cooling rates during casting, indicate a greater creep resistance in the rapidly cooled structure by a factor of three [20]. This was at the expense of a 50% reduction in creep ductility and applied to the high stress regime. Since the effect of microstructure is generally more profound at low applied stresses, it is perhaps reasonable to expect an even greater influence of cooling rate in the service stress regime.

Because solder is generally constrained within a joint, its stress relaxation behaviour is more directly relevant to performance than creep. While the two processes are usually regarded as being mechanistically equivalent, the stress exponent in the stress-strain rate relationship during stress relaxation is often slightly higher ($\simeq 1$) than that measured during creep at the same stress level [21, 22]. For stress relaxation from high strain levels ($> 10\%$) the contribution of anelastic strains may be significant.

5.2. Isothermal fatigue

Like most ductile metals, solders tend to follow the Coffin–Manson relationship under strain controlled fatigue i.e.

$$N_f^{\beta} \Delta\varepsilon_p = C$$

where N_f is the number of cycles to failure, $\Delta\varepsilon_p$ the plastic strain range and β and C are constants. During continuous cycling at room temperature, eutectic solders exhibit single linear relationship between N_f and $\Delta\varepsilon_p$ with a gradient (β) of 0.5 [23, 24] at plastic strain ranges above about 0.5%. At smaller strain range levels β increases [25]. Lead-rich solders also develop

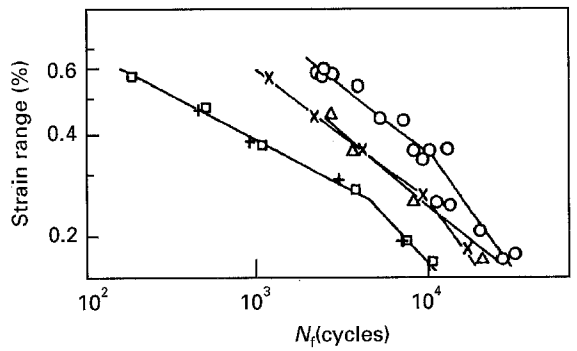

Figure 12 Coffin–Manson plot for a lead-rich solder at various temperatures [26]. $t_r = 0.1$–0.25 s. △ 5 °C; ○ 25 °C; × 50 °C; □ 80 °C; + 100 °C.

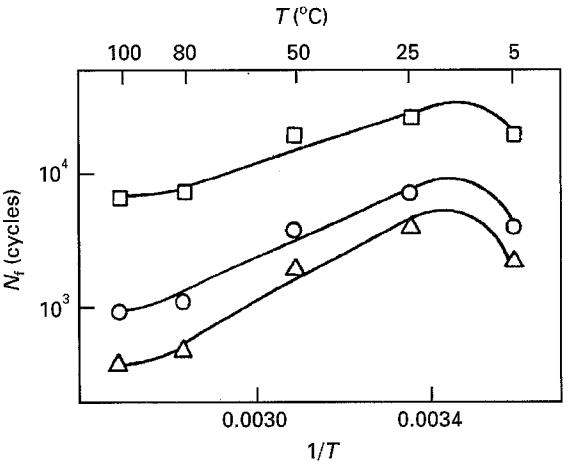

Figure 13 Effect of temperature on fatigue life of a lead-rich solder [26]; t_r is the cycle ramp time (= 0.1–2.5 s). Total strain range □ 0.3%, ○ 0.5%, △ 0.6%.

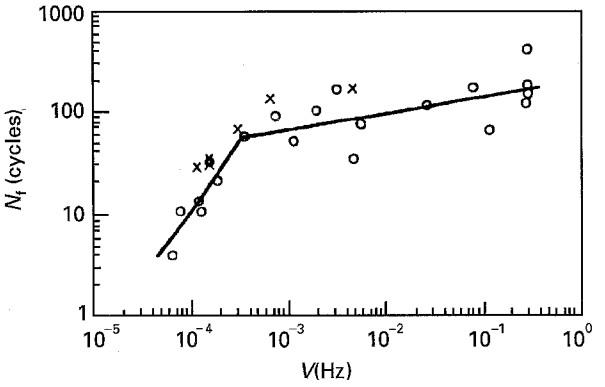

Figure 14 Effect of frequency on fatigue life of a eutectic solder [39]. The small effect of cycles with balanced dwells is also illustrated. ○ continuous cycling (VV); × hold time (⊔⊓⊔⊓).

a deviation from a single linear plot at low strain ranges (Fig. 12) which has been attributed to a fracture mode transition (from mixed to intergranular) and environmental effects [26].

The range of test methods and the definition used to denote failure may have a marked effect on the slope and relative displacement of the Coffin–Manson line [10]. Such an effect is particularly significant for solders where test data are commonly obtained from shear straining and also from actual joint geometries. For example, data from cyclic shear tests using a pin and ring system do not exhibit bilinearity in the Coffin–Manson line at low strain ranges [27]. With such a variation, direct comparison is difficult and values for the constants in the Coffin–Manson expression require close inspection to reveal their relevance.

When attempting to identify the effects of temperature and strain rate (frequency) on the isothermal fatigue performance of solders, it must be appreciated that their influence is very much interrelated. In combination, they govern the extent of time dependent processes that take place. Even during continuous cycling, with a high homologous temperature, these can be significant. While comprehensive data describing the interdependence are unavailable [5, 23, 28], there is considerable evidence that the fatigue lives of eutectic and near-eutectic solders are relatively insensitive to temperature over likely operating ranges (− 50 to 150 °C) [29]. In contrast, lead-rich solders are more affected by temperature, a 95Pb–5Sn alloy exhibiting a reduced endurance with increasing temperature, up to around 150 °C [30]. For another alloy (96Pb–3.5Sn) the fatigue life was a minimum between 88 and 100 °C [31, 32] (Fig. 13).

In general, frequency (i.e. number of cycles per unit time) affects fatigue endurance over an intermediate range which is neither too rapid for time dependent phenomena to be influential nor too slow for them to have saturated. In eutectic solders the critical frequency levels below which frequency has a significant effect upon fatigue life have been identified as 3×10^{-4} Hz and 3×10^{-3} Hz at 35 °C and 150 °C, respectively [23, 33] (Fig. 14). The equivalent strain rates in these tests are one-fifth of the frequency values ($\dot{\varepsilon} = 2\Delta\varepsilon f$). A higher value for the critical frequency (10^{-2} Hz) has been reported for lead-rich solders [26] and this appears insensitive to temperatures between 25 and 80 °C. Eckel [34] has suggested that endurance, N_f, and frequency, f, may be related empirically by

$$N_f = bf^{1-m}$$

where b and m are constants; m has a value of 0.75 for a 95Pb–5Sn solder [34]. However, it must be remembered that it is strain rate, rather than frequency, which is the fundamental parameter influencing material behaviour. For most structural materials, which are usually fatigued at strain ranges below 2%, the trends exhibited by frequency data persist to strain rate. In solders, where strain ranges may exceed 10% this link is less secure.

Apparently conflicting evidence exists with regard to the effect of ageing on fatigue of eutectic solders [5, 6]. Much depends upon the detail of the prior thermal history, the severity of cycling, and whether ageing obliterates the effects of differences in initial microstructures [6, 7].

5.2.1. Effect of dwell periods

Solders in service are rarely subjected to regular continuous cycles but experience dwell periods of several hours or days according to performance demands. Their mechanical hysteresis loops thus contain holds

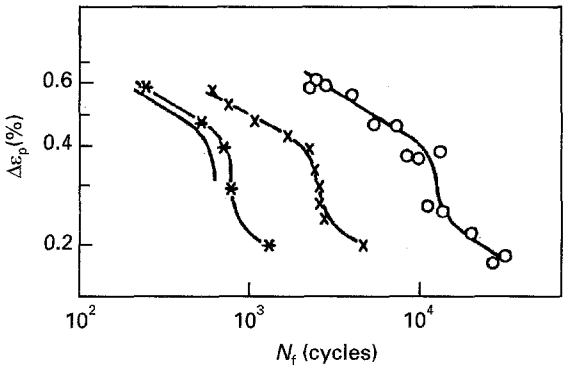

Figure 15 Effect of tensile dwells on endurance of a lead-rich solder [26] at 25 °C, t_r = 1.0–2.5 s. ○ no hold; × 30 s hold; * 360 s hold; —1–10 h, N_f' extrapolated.

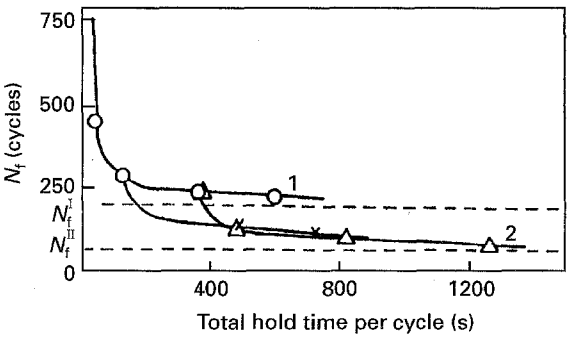

Figure 17 Effect of combined tensile and compressive dwells on the endurance of a lead-rich solder during strain controlled cycling in tension [26]. $\Delta\varepsilon_t$ = 0.75%, 2.5 °C, t_r = 2.5 s. ○ tensile hold time only; × 120 s t_{ht} plus variable t_{hc}; △ 360 s.

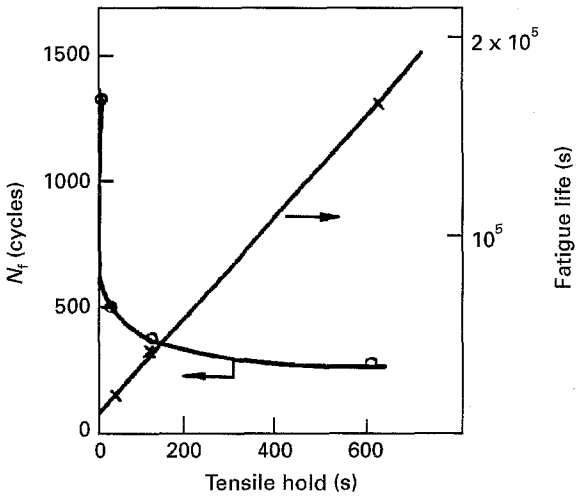

Figure 16 Saturation of the dwell effect on life of a eutectic solder [36] at 25 °C, 1% total strain, ramp 1 s.

at constant strain levels during which stress relaxation may occur and introduce a further factor influencing life. Laboratory tests usually incorporate the dwells at the maximum strain limits since, for other structural alloys, dwells at intermediate levels have been shown to have a less marked effect on endurance [35].

Both eutectic and lead-rich solders have been found to be tensile-dwell sensitive i.e. a significant life debit is observed following fatigue with cycles containing dwells at maximum tensile strain [26, 36]. The reduction in endurance compared with that obtained for continuous cycling may be greater than an order of magnitude (Figs 15 and 16). A saturation in this deleterious effect is usually observed when the dwell duration exceeds about 100 s. Tests in vacuum on lead-rich solder [37] indicate that the nature of the time dependent damage accruing during the dwell is mechanical rather than environmental since the number of cycles to failure is only slightly greater than in air. Grain boundary voids are produced for both solder types after tensile-dwell cycling [37, 38] as for all tensile-dwell sensitive alloys. The considerably greater influence of dwell-containing cycles is an important feature. Even though the overall time per cycle may be similar, strain rates during dwell periods are much slower and more conducive to intergranular damage than those during continuous cycling.

Balanced dwell cycling, i.e. cycling containing hold periods of equal duration at maximum tensile and compressive strain have been shown to be not deleterious to the endurance of eutectic solders [39] (Fig. 14). In lead-rich solders, compressive dwells may accentuate the life debit produced by tensile dwells in tension–tension strain controlled cycling when the dwell at zero strain occurs under compressive stress [26] (Fig. 17). It is expected that unbalanced compressive dwells in fully reversed cycling will not be detrimental to the endurance of solders since the necessary build-up of mean stress requires a high modulus and yield strength [40].

5.3. Thermomechanical fatigue

The earlier description of typical service conditions for soldered joints indicated that the vast majority of failures arose due to the development of cyclic strains induced by temperature fluctuations and a mismatch in thermal expansion coefficients of the material components of the joint. In this example of thermomechanical fatigue (TMF), while instances of substantial temperature variations were cited, even small changes may be significant depending upon the joint size and the degree of mismatch in expansion coefficients. Because of the change in temperature, the material may exhibit quite different characteristics during the course of a single cycle. In particular, the location of any dwell with respect to the current temperature is critical since this governs the extent of time dependent effects. For example, it is estimated that at temperatures greater than 80 °C, stress relaxation will be complete in one minute whereas at below − 55 °C its extent over a period of days will be small [41].

Information regarding the TMF behaviour of solder alloys is limited since most tests involve joint geometries where stress data are difficult to obtain. Lawson [42, 43] has found for lead-rich solder, cycled between tensile strain limits, that hold periods at either extreme are damaging to endurance, although creep cavitation was not produced during the dwells. Continuous cycling between 25 and 80 °C results in a shorter life than isothermal fatigue at 80 °C although this difference tends to disappear at high rates of deformation.

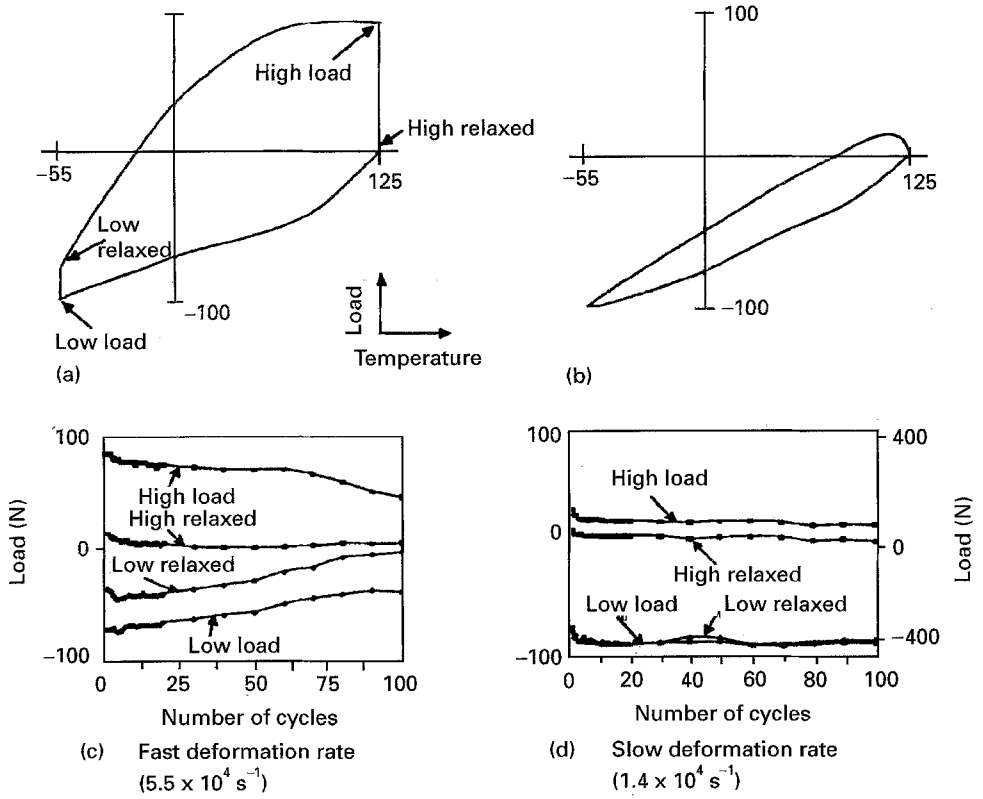

Figure 18 Effect of strain rate on hysteresis loop shape and cyclic strength of a near-eutectic solder [69].

In contrast to isothermal fatigue behaviour, increasing frequency produces a reduction in life for both solder groups [43, 44]. It has been suggested that this is due to the shorter time available for damage to anneal out during cycling. Minimum life was associated with in-phase cycling (temperature and strain 90° apart) and endurance was a maximum with a 270° phase difference. Post-TMF test measurement indicates that the strength of a joint as determined by a torque test, decreases as the number of cycles increases [45, 46]. Strain rate may have a profound effect on the load–strain hysteresis loop (Fig. 18). In particular, peak tensile loads and the extent of stress relaxation are markedly reduced at slow deformation rates [47]. In joint geometries which can be fully instrumented, constitutive modelling of the shear stress–shear strain hysteresis loops gives good agreement with experimental observation [48] (Fig. 19). Measurement of crack areas from interrupted tests suggest a proportionality between log growth rate and log crack length [48].

Mechanistically, the microstructural consequences of TMF are broadly similar to those observed in the less complex deformation processes. Surface roughening occurs due to slip displacement; heterogeneous coarsening of the eutectic microstructure results from high strain cycling and alignment of the lead-rich phase is observed [49, 50]. The coarsened bands tend to be broader than those produced during isothermal fatigue [51] and at deformation rates below $10^{-8}\ s^{-1}$ they follow the cell boundaries while at rates in excess of $10^{-5}\ s^{-1}$ the predominant orientation is along the direction of the imposed shear strain. Having initiated in the coarsened bands, cracks may propagate via the

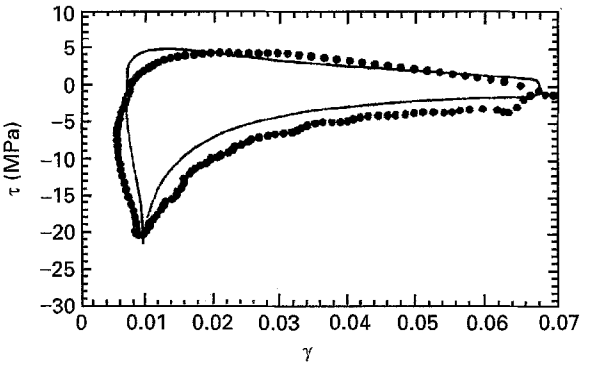

Figure 19 Correlation between predicted and experimental hysteresis loops during TMF (30/130 °C, 24 min triangular cycle) of a eutectic solder (63Sn–37Pb) [48]. ● experimental; — iterated.

lead-rich [49, 50], the tin-rich [52] phases or by interphase separation [53, 54]. Classic fatigue striations have been reported on fracture surfaces of the thermally cycled joints [55].

Evidence regarding the effects of prior ageing on TMF of joints is unclear. Some workers [45, 46] have ascribed early failures to the fracture of intermetallic phases, especially in thin joints. While others [56, 57] contend that ageing proceeds to a stable condition so rendering the initial microstructure irrelevant to the endurance and failure mode. Due to the likelihood of changes in deformation mechanism over the temperature range encompassed by a TMF test, the use of isothermal data to predict TMF performance is suspect. Even in the absence of mechanism changes, the generation of hysteresis loops for TMF from isothermal data is complex [58, 59].

5.4. Crack growth

Cyclic crack growth occurs in solder alloys with the formation of fracture surface striations when local plane strain conditions and Mode 1 crack opening predominate. In joint geometries, the striations may be very fine and require field emission scanning electron microscopy (SEM) for their resolution [60, 61]. It has been suggested [60] that the striation-forming mechanism is that of Laird [62] and Pelloux [63], and that the dominant strain parameter is the equivalent strain as calculated from the von Mises criterion. The most influential factors governing the dominant deformation and fracture mechanisms are strain rate and temperature. Thus at low strain rates (usually low frequencies) totally intergranual fracture may occur under fatigue. For example, Greenwood *et al.* [38] testing a low-tin solder in reverse bending, at a frequency of 5×10^{-2} at room temperature, were able to monitor the accumulation of fatigue damage from interrupted testing. Using gallium as a liquid metal embrittlement agent, the nucleation, growth and coalescence of grain boundary cavities produced by fatigue were observed. Initially, cavity density increased proportionally with the number of applied cycles but subsequently, this rate tailed off. It was proposed that this method might be suitable for evaluating the condition of joints removed from components in service. Laboratory fatigue tests carried out in fluctuating shear tend not to produce fracture surface striations [64]. Ductile dimples, shear markings, granulated features and intergranular failure have been reported.

An intrinstic difficulty with ductile materials, such as solders, is the degree to which equations describing crack growth may be applied. Certainly, elastic fracture mechanics appears inappropriate although data have been presented in these terms [65]. Using thick (11 mm) compact tension (CTS) specimens under fluctuating tension ($R = 0.1$), plots of log growth rate versus log stress intensity range indicate an exponent in the Paris equation of about 3.5. Although crack closure was not detected, an oxide film was produced which was attributed to the rubbing together of mating fracture surfaces. Not surprisingly, the thickness of the oxide increased as the stress intensity range diminished. No striations were observed. Doubts have also been expressed regarding the applicability of the J and ΔJ approaches [66].

In the context of the soldered joint and service conditions, further complications arise [66]. Time-dependent contributions to crack growth arising from creep and its interaction with cyclic damage are unknown. The equivalence between crack growth under a mechanically induced ΔJ and that produced by a thermally induced ΔJ remains to be proven. Further, crack growth usually occurs in shear and non-linear fracture mechanics is poorly developed for Modes II and III opening, even disregarding the likely actual conditions in which they are combined under a multiaxial stress/strain regime. Finally, the joint dimensions of the solder layer in a joint are generally such that "short" rather than "long" crack growth conditions prevail. Life may then be determined by cracks extending an order of magnitude faster than will be expected from conventional long crack growth data and the influence of local microstructure might be considerably enhanced [67].

Satoh *et al.* [60, 61] have employed crack growth data from striation spacing measurements on actual joints. In conjunction with finite element analysis, it was possible to predict life and the location of failure. Integration of growth rate expressions indicated that life was thermally activated and frequency dependent. Other studies [48, 68], involving measurement of load drop and analysis of Coffin–Manson data, suggested that a transition in the value of the activation energy of fatigue at about 100 °C was associated with a change in fracture mode from transgranular to intergranular failure.

5.5. Testing and failure definition

Unlike pressure vessels and gas turbines, joints in microelectronics are cheap and relatively easy to test. Consequently, the available data on solders are more than matched by those for the complete component. While it can be argued that assessing the mechanical performance of an entire joint yields valuable information of direct applicability, in terms of joint dimensions, cooling rate, intermetallics and stress–strain distribution, these advantages are tempered by the highly specific nature of the results. Precise values for stress and strain throughout a joint are usually unknown. The alternative contention is that in order to develop more reliable methods of life prediction and improved performance, by way of better materials, the behaviour of the solder materials themselves under complex service-like conditions should be evaluated in depth and fully understood. The bias in this article is towards the generic approach but with the relative wealth of component data available, it is important to have this comparison in mind.

The bulk of information pertaining to TMF is derived from thermal cycling tests using actual components or simplified test specimens. With the former, heat may be applied to the assembly externally or via power cycling. The mechanical strains develop almost simultaneously from the mismatch in thermal expansion coefficients, or temperature gradients, as previously described. Accelerations in test duration of ten to several hundred times are common although the need to retain predominant failure mechanism remains. Problems with complex stress–strain distributions in actual components may be alleviated using simplified geometries for specimens (Fig. 20). While this also permits monitoring of damage under realistic conditions, determination of mechanical properties is not possible and interrupted testing is necessary [69]. Direct TMF evaluation involves the external application of mechanical stress or strain either in phase or out of phase with temperature variations. Bulk specimens are generally cycled in tension–tension and tend to be massive in comparison to joint dimensions. Extensive mechanical data may be obtained during a test and the specimen is uniformly strained. Simple shear strains may be imposed on joints with a double

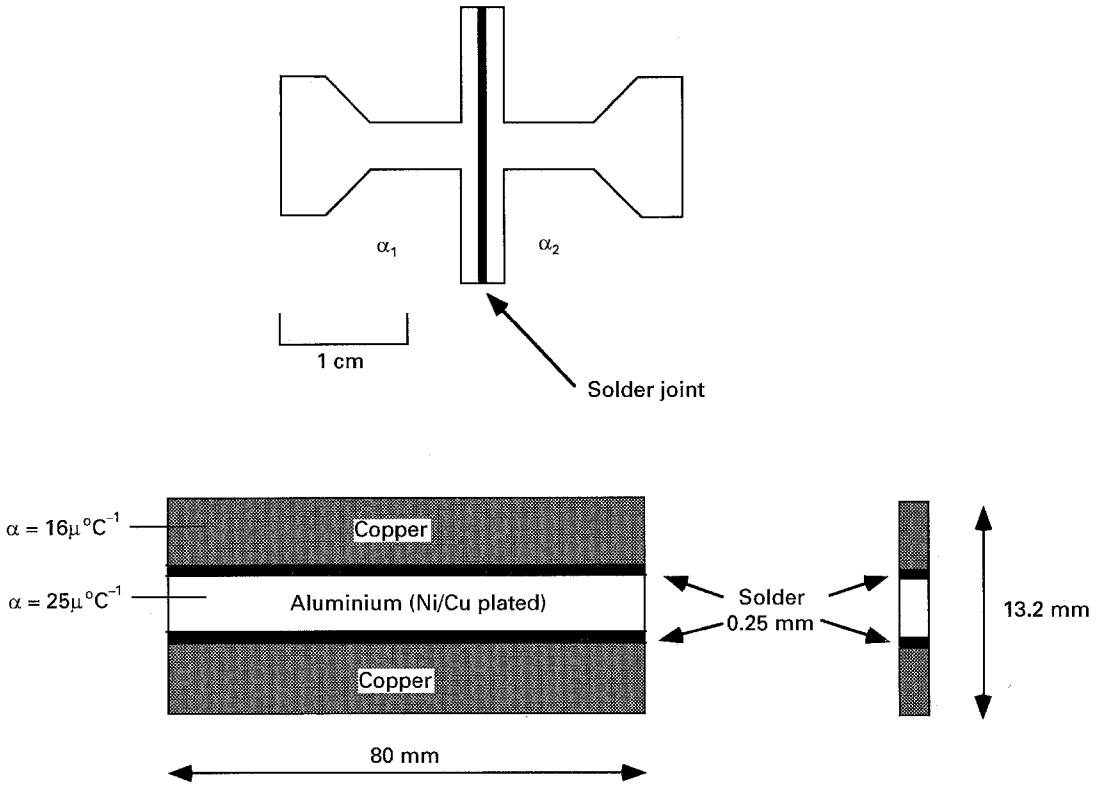

Figure 20 Simplified test specimens for TMF. The shear strains develop as a consequence of thermal cycling and the differences in coefficient of thermal expansion [69].

lap configuration [47] but, overall, the complexity and cost of direct TMF testing represents a significant impediment to its widespread adoption.

In addition to the wide range of test types and specimen geometries, a further feature which impairs comparability of data between sources is the definition employed to denote failure. Variations in the number of cycles to failure of an order of magnitude and changes in slope of Coffin–Manson plots may occur [49, 70]. Failure criteria utilized include onset of a visible crack, the start or a given percentage fall in stress, the ratio of maximum to minimum stress range and a predetermined change in electrical resistance. It should be noted that cracks formed during shear- and tensile-compression strain cycling have different effects on measured stress levels. Also, electrical conductivity tends to break down at much larger crack sizes than are indicated by stress changes (Fig. 21) [64]. Under cyclic shear, crack growth is principally a function of applied plastic shear strain range and is unaffected by crack length [23]. This is in contrast to tension-compression fatigue (Mode I) in which the crack growth rate increases with crack length. An important practical repercussion of this is a strong specimen size effect under shear cycling which arises because crack growth must be longer to cause failure in large specimens. In consequence, the measured fatigue life of a laboratory test piece will be greater than that of a joint under otherwise identical conditions. To a first approximation, crack rates under cyclic shear may be deduced from Coffin–Manson plot effects. Solomon [64] has suggested a scaling factor ($L:D$) which is the ratio of the crack lengths necessary to cause failure in the two specimen geometries.

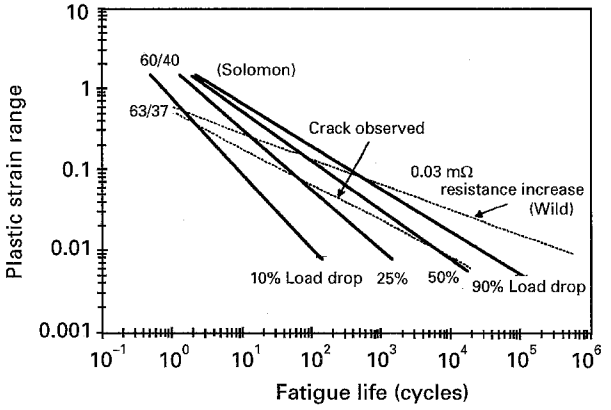

Figure 21 Influence of failure definition on observed fatigue life [49, 70].

6. Life prediction

In comparison to other high temperature structural alloys, such as steels and nickel-base alloys, life prediction for solders in joints is more complex due to the generally higher homologous temperature, the greater degree of microstructural instability and inhomogeneity, the small size of actual components and the relative scarcity of comparable data. Component life estimation involves two stages; the calculation of stress and strain levels and their distribution, and employing that information in a life predictive expression. In the following paragraphs only the second stage is considered, and the applicability to solders of popular methods for high temperature structural alloys is explored.

Approaches based upon stress are generally not appropriate because strain is the operative factor in service. The presence of a stress in an unconstrained configuration would result in gradual creep failure. Strain-based approaches such as Coffin–Manson, or its frequency modified variant, work reasonably well for uniform, constant amplitude, cycling at total strain ranges in excess of about 1% [23, 24]. Some of the plots particularly from lead-rich solders, also exhibit bilinearity [71, 72] which adds uncertainty to the extrapolation of high strain range data to lower strain levels. Englemaier [73] has incorporated total shear strain, instead of plastic shear strain, into the Coffin–Manson expression and obtained a method for first-order life prediction of joints. Strain range partitioning has been a popular method of life prediction for many structural alloys. The method requires a large volume of data from quite complex tests and such information is not generally available for lead-tin solders. Further problems arise due to the difficulty in determining accurate values of inelastic strains in the joint. Soft ductile materials such as solders are not amenable to analysis using linear elastic fracture mechanics and the J-integral may be inappropriate because of the onset of general yielding, the material's instability and the difficulty of measuring crack length [74]. Damage rate equations [75, 76] are unusual amongst life prediction approaches in that they consider the actual mechanisms causing deformation and failure. Integration of expressions for the rate of damage (cracks or cavities) accumulation provides an estimation of life. There is an implicit assumption that the microstructure remains unchanged and also, when extrapolating data, that the dominant failure mechanism is the same in the laboratory (experiment) and the service situation. Clearly such assumptions are quite suspect for the unstable microstructures in solders. There is a pressing need to gain further understanding of the dominant failure mechanisms and to identify the extent, in terms of temperature, strain and strain rate level, over which they prevail.

7. Future solders

Current solders are beset by two fundamental deficiencies: one technical and one environmental. The former is the intrinsic vulnerability to cyclic deformation which is associated with the localization and concentration of damage, giving rise to early crack initiation. Strategies for the amelioration of this problem exist, in principle, and for eutectic alloys involve replacement of the eutectic microstructure with a fine equiaxed grain homogeneous structure. This may be achieved by thermomechanical processing or by appropriate alloy addition. Alternatively, incorporation of a dispersion of second phase particles may prevent growth of the recrystallized bands. In lead-rich solders, where failure is generally intergranular, impurity removal or addition of elements to improve adhesion between grains, or the use of pinning precipitates to inhibit grain boundary sliding, are potential solutions [77]. It has to be borne in mind, however, that current understanding is based upon evidence from simple tests. There is an implicit assumption in the above prescriptions that the dominant-failure mechanism in the composite structure of the joint, experiencing complex stress/strain/time conditions usually in shear, remains unchanged. Moreover, the entire solder joint system has to be considered and the repercussions of the solution to the low fatigue resistance problem on the processing and manufacturing requirements have to be evaluated. Clearly, we still have a great deal to understand!

Since it is uneconomic to recycle the lead content of PCBs, contamination of the environment may arise from its entry into ground water near land-fill sites or into the atmosphere following incineration of defunct electronic equipment. With anti-lead legislation expected in the none-too-distant future, there exists strong pressure to identify lead-free alternatives to current solders. The requirements for the replacements are wide-ranging and the choice is not large. Liquidus and solidus temperatures should be low and close together. Common metals and metallizations should be wetted by the alloy which preferably should be compatible with existing fluxes. In addition to stability and corrosion resistance, compounds forming during joining must possess adequate mechanical properties. Finally, replacements need to be economically available and, of course, not intrinsically toxic themselves.

Of the low melting point elements, cadmium, thallium and mercury are toxic, the alkali earth metals are highly reactive and gallium, indium and bismuth not available in sufficient quantities. Tin appears the ideal candidate as the basis for the new generation of solders. Alloys containing bismuth, zinc, silver, gold and copper have been investigated [1] and those between tin and 2 or 3.5 wt % silver, and tin and 0.7 wt % copper found to be the most promising. These rankings are based mainly upon processing parameters. The extensive mechanical evaluation necessary to assess structural integrity remains to be performed.

8. Conclusions

Solders are under pressure from two separate sources. In the short term, the ever-increasing demands for improved performance and continued miniaturization is focusing attention on their ability to provide structural integrity. Since the consequences of joint failure may be potentially as catastrophic as with more conventional large-scale structures, the comparative lack of progress in validating design is disturbing. The tension between mechanical conservatism in design and performance requirements is increasing rapidly.

In the medium term, it seems inevitable that conventional lead-containing solders will be replaced by their more environmentally-friendly equivalents. Even when the prime candidates have been selected and appraised in terms of processability and with an application temperature below 200 °C, the problem of structural integrity will remain. Perhaps it is timely for materials engineers to anticipate this since we are largely in a vacuum of knowledge and understanding

on this aspect. Even more dramatic departures from the use of metallic solders are possible with the increased employment of conducting polymeric adhesives [78]. Irrespective of the nature of the connecting medium, the problem of structural integrity will require a solution.

Acknowledgements

The author would like to express his sincere thanks to his colleagues, Reinhold Hermann, Honggen Jiang and Colin Gagg, for their assistance in the preparation of this article.

References

1. J. H. VINCENT and G. HUMPSTON, *GEC J. Res.* **11** (1994) 76.
2. K. R. KINSMAN in "Solder mechanics – a state of the art assessment", edited by D. R. Frear, W. B. Jones and K. R. Kinsman (The Metals Society, Electronic, Magnetic and Photonic Materials Division 1, 1990) XIX.
3. J. SOOVERE, B. V. DANDAWATE, G. A. GARFINKEL, N. ISIKBAY and D. S. STEINBERG, Report AFWAL-TR-87-3048, Flight Dynamics Laboratory, Wright Patterson AFB, OH (1987).
4. H. J. FROST, in "Solder joint reliability, theory and applications", edited by J. H. Lau (van Nostrand Reinhold, New York, 1991) p. 266.
5. E. C. CUTIONGCO, S. VAYNMAN, M. E. FINE and D. A. JEANNOTTE, *J. Electronic Packaging* **112** (1990) 110.
6. M. A. WHITMORE, P. G. HARRIS, K. S. CHAGGAR and A. C. CHILTON, NEPCON Europe, Birmingham, March 1990.
7. C. GAGG, private communication (1994).
8. B. T. LAMPE, *Welding J. Research Supp.* **55** (1976) 3305.
9. D. R. FREAR, J. B. POSTHILL and J. W. MORRIS Jr, *Metall. Trans.* **20A** (1989) 1325.
10. S. VAYNMAN and M. E. FINE, "Solder joint reliability, theory and applications", edited by J. H. Lau (van Nostrand Reinhold, New York, 1991) 333.
11. E. LEVINE and J. ORDONEZ, *IEEE Comp. Hybrids Manufact. Tech.* **CHMT-4** (1981) 515.
12. D. FREAR, *J. Met.* **40** (1988) 18.
13. A. D. ROMIG, Y. A. CHANG, J. J. STEPHENS, D. R. FREAR, V. MARCOKER and C. LEA, "Solder mechanics – a state of the art assessment", edited by D. R. Frear, W. B. Jones and K. R. Kinsman (The Metals Society, Electronic, Magnetic and Photonic Materials Division 1, 1990) 29.
14. K. P. JEN and J. N. MAJERUS, *J. Engng Mater. Technol.* **113** (1991) 475.
15. B. P. KASHYAP and G. S. MURTY, *Res. Mechanica.* **3** (1981) 131.
16. K. KAWASHIMA, T. ITO and M. SAKURAGI, *J. Mater. Sci.* **27** (1992) 6387.
17. R. ARROWOOD, A. MUKHERJEE and W. B. JONES, in "Solder mechanics – a state of the art assessment", edited by D. R. Frear, W. B. Jones and K. R. Kinsman (The Metals Society, Electronic, Magnetic and Photonic Materials Division 1, 1990) p. 107.
18. B. P. KASHYAP and G. S. MURTY, *J. Mater. Sci.* **18** (1983) 2063.
19. E. PINK, A. MARQUEZ and A. GRINBERG, *Scripta Metall.* **15** (1981) 191.
20. C. GAGG, W. J. PLUMBRIDGE and R. HERMANN, unpublished work.
21. A. E. GECKINLI and C. R. BARNETT, *Scripta Metall.* **8** (1974) 115.
22. J. P. CLECHE and J. A. AUGIS, IEPS, Dallas, Nov 1988, p. 305.
23. H. D. SOLOMON, in "Electronic packaging: materials and processes", edited by J. A. Sortell (ASM, Metals Park, OH, 1985) p. 29.
24. G. ENGBERG, L. E. LAVSSON, M. NYLEN and H. STEEN, *Brazing and Soldering* **11** (1986) 62.
25. K. BOCE, K. BAE, A. F. SPRECHER, D. Y. JUNG and H. CONRAD, in Proceedings Second ASM International Electronic Materials and Processing Congress, edited by W. T. Shieh, 1989, p. 264.
26. S. VAYNMAN, M. E. FINE and D. A. JEANNOTTE, *Metall. Trans.* **19A** (1988) 1051.
27. R. SANDSTRÖM, J. O. ÖSTERBERT and M. NYLEN, *Mater. Sci. Tech.* **9** (1993) 811.
28. M. KITANO, T. SHIMIZU and T. KUMAZAVA, *Current Japanese Mater. Res.* **2** (1987) 235.
29. P. M. HALL, *IEEE Comp, Hybrids Manufact. Tech.* IEEE CHMT-7, 405 (1984).
30. D. FREAR, D. GRIVAS, M. MCCORMACK, D. TRIBULA and J. W. MORRIS Jr, in Proceedings of the Effect of Load and Thermal Histories on Mechanical Behaviour Symposium, edited by P. K. Liaw and T. Nicholas, 1987, p. 113.
31. H. S. RATHORE, R. C. YIH and A. R. EDENFIELD, *J. Test Eval.* **1** (1978) 170.
32. S. VAYNMAN, in Proceedings of the Intersociety Conference on Thermal Phenomena in Electronic System (I-Therm II) IEEE, 1990, p. 16.
33. H. D. SOLOMON, ASTM STP 942, edited by H. D. Solomon, G. R. Halford, L. R. Kaisand and B. N. Leis, 1988, p. 342.
34. J. F. ECKEL, *Proc. ASTM* **51** (1957) 745.
35. H. L. BERNSTEIN, in "Low cycle fatigue and life predictions", edited by C. Amzallag, P. Rabble and B. N. Leis (ASTM STP 770, Philadelphia, 1982) p. 105.
36. S. VAYNMAN and M. E. FINE, in Proceedings of the 2nd ASM International Electronic Materials and Processing Congress, edited by W. T. Shieh (1989) p. 255.
37. R. BERRICHE, S. VAYNMAN, M. E. FINE and D. A. JEANNOTTE, in Proceedings of the 3rd Annual Electronic Packaging and Corrosion in Microelectronics Conference, edited by M. E. Nicholson (ASM, International, 1987) p. 169.
38. P. J. GREENWOOD, T. C. REILEY, V. RAMAN and J. K. TIEN, *Scripta Metall.* **22** (1988) 1465.
39. H. D. SOLOMON, in 38th Electronic Components Conference, IEEE (1988) p. 7.
40. W. J. PLUMBRIDGE, in "High temperature fatigue properties and prediction", edited by R. P. Skelton (Elsevier Applied Science, London, 1987) p. 117.
41. D. R. FREAR, in Proceedings of the 40th ECTC Conference Las Vegas, NV, 1990, p. 510.
42. L. R. LAWSON, M. E. FINE and D. A. JEANNOTTE, in Third International Conference on Fatigue and Fatigue Thresholds, Charlottesville, June 1987, edited by R. O. Ritchie and E. A. Starke (EMAS Ltd, UK, Vol II, 1987) p. 1143.
43. L. R. LAWSON, Ph.D. Thesis, North Western University (1989).
44. D. R. FREAR, *IEEE Comp. Hybrid Manufact. Tech.* IEEE CHMT-4, 1981, p. 492.
45. H. N. KELLER, *ibid.* (1981) p. 132.
46. L. P. KARJALAINAN, R. H. RAUTIOAHO, S. A. JARVENPAA, R. RIKOLA and J. VAHAKANGAS, *Brazing and Soldering* **15** (1988) 15, 37.
47. D. R. FREAR, in Proceedings of the 40th ECTC Conference, Las Vegas, NV (1990) p. 518.
48. P. L. HACKE, A. F. SPRECHER and H. CONRAD, in "Thermal stress and strain in microelectronics packaging", edited by J. H. Lau (Van Nostrand Reinhold, New York, 1993) p. 467.
49. R. N. WILD, *Welding Res. Suppl.* **51** (1972) 521s.
50. W. M. WOLVERTON, *Brazing and Soldering* **16** (1987) 33.
51. D. TRIBULA, D. GRIVAS, D. R. FREAR and W. J. W. MORRIS Jr, *Welding Res. Supp.* (1989) 4045.
52. D. FREAR, D. GRIVAS and J. W. MORRIS Jr, *J. Electr. Mater.* **17** (1988) 171.
53. E. R. BANGS and R. E. BEAL, *Welding Res. Suppl.* (1975) 377s.
54. K. G. SCHMITT-THOMAS and S. WEGE, *Brazing and Soldering* **11** (1986) 27.
55. M. HARADA and R. SATOH, in Proceedings of the 40th ECTC Conference Las Vegas, NV (1990) p. 510.

56. D. R. FREAR, D. GRIVAS, and W. J. W. MORRIS Jr, *J. Electr. Mater.* **18** (1989) 671.
57. E. A. WRIGHT and W. M. WOLVERTON, in Proceedings of the 34th Electronics Components Conference **34** (1984) 149.
58. R. P. SKELTON, *Fatigue and Fracture of Engineering Materials and Structures* **17** (1994) 479.
59. T. GOSWAMI and W. J. PLUMBRIDGE, in International Conference on Mechanical Behaviour, ICM 6, Japan (1991) p. 85.
60. R. M. SATOH, "Solder joint reliability, theory and applications", edited by J. H. Lau (van Nostrand Reinhold, New York, 1991).
61. R. M. SATOH, K. OSHIMA and K. ARAKAWA, in Proceedings of the Conference of Japan Institute of Metals (1988) p. 144.
62. C. LAIRD and G. C. SMITH, *Phil. Mag.* **7** (1962) 847.
63. R. M. N. PELLOUX, *Trans. Amer. Soc. Met.* **61** (1969) 281.
64. H. D. SOLOMON, "Solder joint reliability, theory and applications", edited by J. H. Lau (van Nostrand Reinhold, New York, 1991) p. 406.
65. P. K. LIAW, W. A. LOGAN and M. A. BURKE, *Scripta Metall.* **23** (1989) 747.
66. S. MAJUMDAR and W. B. JONES, "Solder mechanics – a state of the art assessment", edited by D. R. Frear, W. B. Jones and K. R. Kinsman, p. 273.
67. S. SURESH and R. O. RITCHIE, *Int. Metall. Rev.* **29** (1984) 445.
68. Z. GUO, A. F. SPRECHER and H. CONRAD, in 41st Electronic Components and Technology Conference (1991) p. 658.
69. D. R. FREAR, "Solder mechanics – a state of the art assessment", edited by D. R. Frear, W. B. Jones and K. R. Kinsman, p. 191.
70. H. D. SOLOMON, *Trans.* ASME, *J. Electr. Packaging* **111** (1989) 75.
71. S. VAYNMAN, in Proceedings of the 40th Electronic Components and Technology Conference, Las Vegas (1990) p. 505.
72. A. ZUBELEWICZ, R. BERRICHE, L. M. KEER and M. E. FINE, *Trans. ASME, J. Electr. Packaging* **111** (1989) 179.
73. W. ENGLEMAIER, *IEEE Trans. CHMT* **6** (1983) 232.
74. B. I. SANDOR, "Solder mechanics – a state of the art assessment", edited by D. R. Frear, W. B. Jones and K. R. Kinsman, p. 363.
75. S. MAJUMDAR and P. S. MAIYA, *Canadian Met. Q.* **18** (1979) 57.
76. P. S. MAIYA and S. MAJUMDAR, *Scripta Metall.* **13** (1979) 485.
77. J. W. MORRIS Jr and Z. MEI, "Solder mechanics – a state of the art assessment", edited by D. R. Frear, W. B. Jones and K. R. Kinsman, p. 239.
78. M. FENNER, *Electr. Prod.* **24** (1995) 25.
79. T. J. KILINSKI, J. R. LESNIAK and B. I. SANDOR, "Solder joint reliability, theory and applications", edited by J. H. Lau (van Nostrand Reinhold, New York, 1991) p. 384.
80. W. ENGELMAIER, *IEPS* (1984) 360.
81. C. A. HARPER, "Handbook of materials and processes for electronics" (McGraw-Hill, New York, 1970).
82. L. T. GREENFIELD and P. G. FORRESTER, "The Properties of Tin Alloys" (International Tin Research Institute, Publication No. 155, 1947).
83. G. V. CLATTERBAUGH and H. K. CHARLES Jr, in Proceedings of the 35th IEEE Electronic Components Conference, Washington DC (1985) p. 60.
84. E. E. KLUIZENAAR, *Soldering and Surface Mount Technol.* **4** (1990) 27.
85. C. G. SCMIDT, in Proceedings of the 39th Electronic Components Conference (1989) p. 253.
86. B. SUBRAHMANYAM, *Trans. Japan Inst. Met.* **13** (1975) 89.

Received 15 May
and accepted 19 October 1995